

Load Frequency Control by Speed Governors of Two-Area Power System using Digital Controller with Deadbeat Approach

KARTIK CHANDRA PATRA*, ASUTOSH PATNAIK

Department of Electrical Engineering
C.V. Raman Global University, Bhubaneswar, Odisha 752054, INDIA

*Corresponding Author:
ORCID ID: 0000-0002-4693-4883

Abstract: - The primary objective in a power system is to maintain a stable supply of both active and reactive power during steady-state operation. This involves generating and delivering power reliably across an interconnected network while ensuring economic efficiency, and keeping voltage and frequency within acceptable limits.

To achieve the goals of minimizing frequency deviation, reducing steady-state error, and ensuring the fastest response time, various models and controllers have been explored and tested in the context of Load Frequency Control (LFC). After thorough evaluation, a suitable and relatively general model was selected, and tests were conducted using this system model.

In practice, problems occur when power demand exceeds the generated power. Variations in real power primarily impact the system frequency, which is also influenced by deviation in voltage magnitude. With the expansion of interconnected power systems, LFC has become increasingly important. Controllers in these interconnected systems play a important role in maintaining both frequency and voltage magnitude within specified permissible limits in response to small changes in load demand.

Building on a clear understanding of various models—such as a two-area interconnected power system using both conventional and intelligent controllers, a robust PID controller for a single-area reheat thermal power plant optimized with Elephant Herding Optimization, and a two-area LFC system with graphical user interface integration—these systems were tested in an autonomous state to evaluate their responses during transient and steady-state oscillations. The steady-state oscillations were effectively stabilized using a high-frequency, deterministic dither signal. Finally, stabilization through the high-frequency signal combined with a digital deadbeat control approach was tested, aiming to achieve a transient-free, ripple-free response with zero steady-state error in the shortest possible time.

Key-Words: Load Frequency Control (LFC), Interconnected Power System, Automatic Generation Control (AGC), Area Control Error (ACE), Tie Lines (TL).

Received: March 21, 2025. Revised: July 25, 2025. Accepted: August 27, 2025. Published: November 1, 2025.

1 Introduction

A power system can be defined by three key elements: voltage, load flow, and nominal frequency. Any disturbance in one of these, such as changes in load flow configuration, can cause faults and place the power system control in a critical state. Active power is controlled/regulated and monitored with Load Frequency Control (LFC), while reactive power is mainly controlled/regulated by the Automatic Voltage Regulator (AVR), which adjusts the generator excitation to maintain voltage levels and manage reactive power flow. Additional methods include taking reactive power compensation devices such as shunt capacitors and reactors, as well as using regulating transformers. This approach ensures the reliable and economical generation and delivery of power within an interconnected system while keeping voltage and frequency within permissible limits.

To achieve our goal, it is essential to have a clear knowledge of the various components and processes

involved, as outlined above. One of the most popular control strategies that comes to mind is Load Frequency Control (LFC), known for its simplicity, ease of implementation, low cost, robustness, and decentralized nature.

LFC plays a vital role in power system operation by sustaining a stable system frequency and ensuring power balance between different areas [1]. The primary frequency control is exercised by the governor, which responds immediately—within seconds. When the frequency drops, indicating a generation deficit, the speed governor increases the mechanical power input to the turbine.

Automatic Generation Control (AGC), or Secondary frequency control uses a centralized controller to regulate the Area Control Error (ACE), which is calculated as $ACE = \Delta P$ (tie-line power error) + $B \cdot \Delta f$ (frequency deviation). The AGC sends control signals to generators, typically by adjusting the governor set points, to restore the frequency to

its standard value (e.g., 50 or 60 Hz) and maintain scheduled tie-line power exchanges between control areas.

This process requires continuous monitoring of system load and frequency, which serve as indicators of the balance between generation and demand. Generators synchronized to the grid automatically adjust their fuel input or excitation to increase or decrease power output in real time, ensuring total generation matches the load.

AGC is a closed-loop control system that implements Load Frequency Control (LFC) by adjusting generator outputs to counteract frequency deviations caused by alteration in load. The feedback mechanism within AGC continuously monitors tie-line power flow and system frequency. Based on this feedback, AGC generates control signals that are sent to generators to adjust their power output accordingly.

An important element in this process is real-time implementation. Accurate, real-time measurements of system frequency, tie-line power, and other relevant parameters are essential, making the quality and reliability of sensors critical.

To process these measurements and generate precise control signals, modern control algorithms such as adaptive control, optimal control, and fuzzy logic control are employed. These algorithms aim to minimize errors and improve control accuracy, all of which require real-time operation.

Additionally, fast and reliable communication systems are necessary to transmit control signals from the AGC to the generators without delay.

At the core of the system are the governor and turbine controls. The control signals adjust these mechanisms to regulate generator power output effectively.

Finally, given the complexity of the system, challenges inevitably arise, prompting the need for effective solutions. As we embark on this exploration, we focus on examining various models, particularly considering the time required for operation and execution, with an emphasis on achieving the fastest possible response.

Facing these challenges, one promising solution lies in LFC strategies for Renewable Energy-Based Hybrid Power Systems. According to [1], where the authors surveyed 110 relevant articles, a hybrid power system combines renewable energy power plants with conventional power plants. The renewable side often generates non-sinusoidal power, leading to power quality issues such as poor settings and higher transient content. The main challenge in such hybrid systems is managing frequency variations caused by this integration. Proper LFC design is essential to ensure the

dependable and efficient operation of these power systems.

With the expansion of interconnected systems, LFC has become increasingly important. Controllers in these networks are responsible for maintaining frequency and voltage within permissible limits despite small deviation in load demand [2]. Even slight deviations from the standard frequency of 50 Hz or 60 Hz can damage appliances like AC motors and electric clocks. For turbines specifically, operating outside a strict frequency range—below 47.5 Hz or above 52.5 Hz—can lead to blade damage, emphasizing the critical need to maintain tight frequency limits [3].

Considering this perspective, we delve into the vast complexity of interconnected power systems, where hundreds of components must work in synchronism. A minor disturbance in any parameter can destabilize the system and potentially cause catastrophic failure. In this context, the work titled “Implementation of Graphical User Interface (GUI) for Single Area Load Frequency Control” [4] is notable, as it facilitates MATLAB-based optimization for multi-area systems. Their model includes turbine, governor, and load components within the generator power system.

Given the system’s complexity, we have decided to test several models and approaches to advance towards the real-time application of LFC as intended.

In [5], a two-area power system was proposed where each area includes a turbine, generator, and governor. The authors simulated parameters to obtain steady-state responses for both single and dual areas and developed a GUI to enhance parameter control and time-based simulations. They observed that to achieve zero frequency deviation, the Automatic Generation Control (AGC) requires a longer settling time, necessitating a higher AGC gain [5].

Various controllers, including PI and fuzzy logic, have been tested in two-area power systems. It was found that fuzzy controllers outperform PI controllers by offering shorter settling times and reduced overshoot, thereby better maintaining constant frequency [6].

In [7], a multi-area power system was simulated to know the impact of disturbances in each area and evaluate the performance of proposed controllers in frequency regulation across the network. The case studies highlighted that the distribution of active and reactive power sources in each region greatly influences frequency control. The proposed fuzzy logic controllers, with optimized control coefficients, demonstrated the ability to minimize transient oscillations and stabilize the system in the shortest possible time. Specifically, in a two-area

power system case study, the fuzzy controller showed superior performance in frequency recovery compared to PID controllers.

In [8], the tuning of a PID controller for LFC in a single-area reheat thermal power plant is presented using Elephant Herding Optimization (EHO) technique. The study highlights the superiority of EHO-based PID tuning compared to other methods such as Particle Swarm Optimization (PSO), Genetic Algorithm (GA), and Differential Evolution (DE).

In [9], a robust LFC strategy for hybrid microgrids is proposed using Type-3 Fuzzy Logic (T3-FL) to handle stochastic variations. This approach addresses challenges posed by renewable energy sources like wind and solar, which introduce power fluctuations and frequency deviations that can affect system stability. The T3-FL controller employs online adaptation of membership functions and enhanced computational capacity to manage uncertainties in renewable generation and load variations. The results demonstrate that the T3-FL controller outperforms traditional PID and other conventional controllers. However, the study does not address how Limit Cycles (LC) are avoided, suppressed, or eliminated, nor does it report on response time, transient behavior, or steady-state ripple content. Due to these gaps, the scheme may not be fully suitable for real-time applications alongside AGC. In contrast, our proposed work aims to tackle these issues in a two-area power system by offering a method that quench limit cycles while providing transient-free, ripple-free performance with no steady-state error and faster response through digital control based on a deadbeat approach.

In [10], a comprehensive analysis of LFC in multi-area power system networks is depicted, exploring various control schemes including optimal control, variable structure control, self-tuning, and adaptive control under classical, robust, and soft computing frameworks. The study concludes that soft computing methods outperform other control techniques in this context.

In [11], a specialized study examines the influence of exciter and governor parameters on forced oscillations in power systems. It highlights that forced oscillations caused by control system malfunctions or improper parameter settings have increased in frequency. Proper tuning of exciter and governor parameters is critical for sustaining system stability. While simulation studies focus on small transient disturbances or step changes to determine optimal parameters, existing optimization algorithms fall short in effectively fine-tuning parameters to mitigate forced oscillations. Identifying the most sensitive parameters within these control models is vital to maintaining the stability during large,

sustained disturbances. The research underscores the complexity of this task, highlighting it as a particularly challenging and demanding endeavor to implement.

In [12], Load Frequency Controllers (LFC) considering the integration of renewable energy into power systems are presented. LFC, or AGC, remains one of the fundamental daily operations in both modern and traditional power systems. The primary objectives of LFC are to maintain power balance among interconnected areas and to regulate tie-line power flows. Since electric power cannot be stored in large quantities, production must continuously match consumption, making this balance critical for effective power system management. The growing penetration of renewable energy sources has introduced new challenges, necessitating the development of more advanced and adaptive control strategies. The literature reflects this shift, presenting a range of controllers—from conventional approaches to hybrid models that incorporate artificial intelligence techniques alongside traditional methods.

One such advanced technique is the Model Predictive Control (MPC) strategy. MPC is an AI-based algorithm that sequentially optimizes manipulated variables by predicting the system's future behavior, making it one of the leading advanced control methods [13, 14, 15].

Load frequency control has long addressed challenges such as governor backlash nonlinearities. In [16], LFC for interconnected power systems considering governor backlash nonlinearity is discussed, with the control goal of eliminating frequency deviations and tie-line power errors at steady state. Interconnected areas exchange power through tie-lines, which support contractual energy sharing and provide assistance during abnormal conditions. When a load change occurs in one area, it leads to imbalances in system frequency and deviations from the scheduled tie-line power flow. LFC corrects these imbalances using an error signal known as the Area Control Error (ACE). The conventional industry practice involves using the integral of ACE as the primary control signal [17–31].

Stability analysis and system design are often performed using established methods such as the Lyapunov stability method [32]. Harmonic balance and characteristic equations are applied to evaluate Limit Cycles (LC) [33–36]. In the design of Load Frequency Control for interconnected power systems, a variety of decentralized control schemes have been implemented, including variable structure control [21–23], traditional PI/PID controllers, and fuzzy logic controllers [25–30].

One notable decentralized approach is the Decentralized Biased Controller for Load Frequency Control of Interconnected Systems considering governor dead-band/backlash nonlinearities [17], which is regarded as an effective option. It is well recognized that many LFC schemes fail to achieve satisfactory control performance due to the presence of dead-band/backlash nonlinearities in governors. These nonlinearities are inherent to governors and cause unexpected, self-sustained oscillations—limit cycles—in area frequency and tie-line power responses during transients, which must be suppressed [16, 17]. The need to quench or suppress these limit cycles has been addressed in previous works [34, 37]. The proposed work builds upon these efforts with further refinement and improvement to effectively handle these challenges. As discussed clearly in [16,17], the dead band/backlash nonlinearity present in the governor causes self-sustained oscillations, known as limit cycles (LC), which must be eliminated to ensure stability in interconnected power systems through Load Frequency Control (LFC). We propose a method to quench or suppress these limit cycles, enhanced further by a deadbeat control approach, enabling real-time application.

Realizing real-time LFC with Automatic Generation Control (AGC) requires a combination of advanced control techniques, reliable communication systems, and precise system measurements to maintain stability and power balance amid changing load demands and system dynamics.

In [38], tie-line bias control is shown to facilitate power exchange between interconnected areas to manage load dynamics. However, this approach presents challenges since load variations in one area cause frequency deviations and power irregularities in all interconnected areas, which is undesirable.

With the increasing demand for electrical power and the alarming depletion of fossil fuels, the shift toward green energy is crucial. Renewable Energy Sources (RESs) integrated with the power grid are seen as a promising solution [39]. Nevertheless, due to their intermittent nature and lack of redundancy, RESs can introduce instability into the power system, making control and stabilization more challenging [40, 41]. As RESs become an integral part of the expansive power system, improving LFC and enhancing its performance becomes imperative. Several challenges threaten power system stability when there is an imbalance between generation and load demand [41]. To address these issues, advanced control techniques such as Optimal Control, Robust Control, Adaptive Control, Model Predictive Control, Intelligent Control, Fuzzy Control, and Type-3 Fuzzy Control are often employed.

In this work, we adopt a digital control strategy to tackle these challenges, including parameter uncertainties in load characteristics and generator dynamics. Specifically, we apply load frequency control in a two-area power system using a digital control method based on a deadbeat approach.

The primary objective of LFC is to maintain a stable and consistent system frequency and tie-line power exchange by adjusting generator output to meet real power load changes. Ideally, LFC achieves a steady-state system where power generation matches load demand, ensuring power quality, system stability, and uninterrupted electricity delivery within acceptable frequency and phase limits.

Dead band/backlash nonlinearities in governors tend to cause unexpected, sustained oscillations in area frequency and tie-line power transient responses [16]. These sustained oscillations, known as limit cycles, can be quenched by signal stabilization techniques [34], or suppressed via pole placement methods using state feedback—either through arbitrary pole selection or optimal feedback gain design [37].

The work is organized as follows: Section 1 introduces the topic and provides a comprehensive review of existing research. Section 2 selects an appropriate mathematical model and validates it through preliminary testing. Section 3 focuses on predicting and analyzing limit cycles caused by dead band/backlash nonlinearities in an autonomous state. Section 4 presents methods for signal stabilization or suppression of limit cycles using high-frequency deterministic signals—preferably at frequencies more than ten times that of the limit cycles [34, 37, 42, 43, 44, 46]—implemented with the MATLAB SIMULINK toolbox. Section 5 details the digital control strategy based on the deadbeat approach [45]. Finally, Section 6 offers concluding remarks, highlighting the novelty of the work and suggesting directions for future research.

2 Selection of a suitable model for load frequency control (LFC) of interconnected power system with governor backlash nonlinearities

During literature survey a few models caught our attention to examine and test by simulation with the use of SIMULINK Tool Box of MATLAB software. The test is conducted for all selected models keeping the models without backlash nonlinearity, so that the sustained oscillations (LC) can be avoided and the performance of LFC can be tested to ensure right performance.

If the preliminary test indicates that Δf (frequency deviation) or $\Delta \omega$ (angular frequency

deviation) has a non-zero value, a follow-up test [38] may be conducted to assess any resulting power loss. Fig. 1 illustrates the block diagram used to evaluate the correlation between frequency deviation (Δf) and power loss deviation (ΔPL).

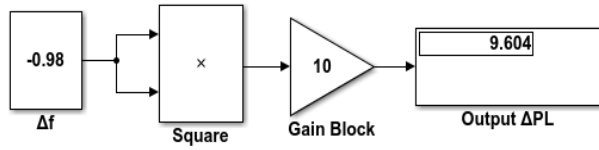


Fig. 1 Block Diagram representation of finding the correlation between Δf (deviation in frequency) and ΔPL (deviation in power loss).

In this setup, the system first measures or receives the frequency deviation signal (Δf), representing the deviation from the nominal system frequency. This signal is then squared (Δf^2) to reflect the assumed quadratic relationship between frequency deviation and power loss. This assumption is based on the principle that power loss, like that in transmission lines, often varies with the square of a dependent variable—in this case, frequency deviation. The squared value is multiplied by a constant gain factor, a , which determines the sensitivity of the power loss to the frequency deviation. The resulting output, ΔPL —typically expressed in megawatts (MW)—quantifies the change in power loss due to the frequency deviation. The relationship is modeled mathematically as:

$$\Delta PL = a \times (\Delta f)^2$$

Here, a is a system-specific constant that defines how strongly frequency deviations influence power losses, potentially due to changes in system loading, generator performance, or power flows. Fig. 2 presents a graphical representation of the relationship between Δf and ΔPL .

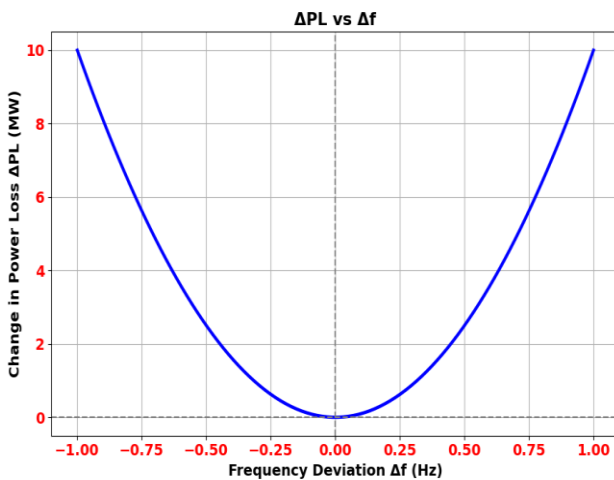


Fig. 2 Graphical plot showing the relation between Δf and ΔPL

Numerical Example:

Consider a scenario of a power system operates at a nominal frequency (f_0) of 50 Hz. A disturbance (e.g., load change or generator outage) causes a frequency drop (f) to 49.6 Hz. To assess the associated power loss using a known sensitivity relationship between frequency deviation and power loss, the following method is used.

The frequency deviation is given by

$$\Delta f = f - f_0 = 49.6 \text{ Hz} - 50 \text{ Hz} = -0.4 \text{ Hz}$$

Let the sensitivity constant a to be 10 MW/Hz².

$$\begin{aligned} \Delta PL &= 10 \text{ MW/Hz}^2 \times (-0.4 \text{ Hz})^2 \\ &= 10 \times 0.16 = 1.6 \text{ MW} \end{aligned}$$

2.1 Model of “Implementation of Graphical User Interface for Single Area Load Frequency Control”, [4] is considered. Fig. 3(a) shows the block diagram representation with the use of SIMULINK Tool Box. Fig. 3(b) shows output (Δf) of Fig. 3(a) [4], the response shows a transient continues up to 400 seconds and the steady state value is zero which implies proper of LFC so that the frequency remains at its nominal value:

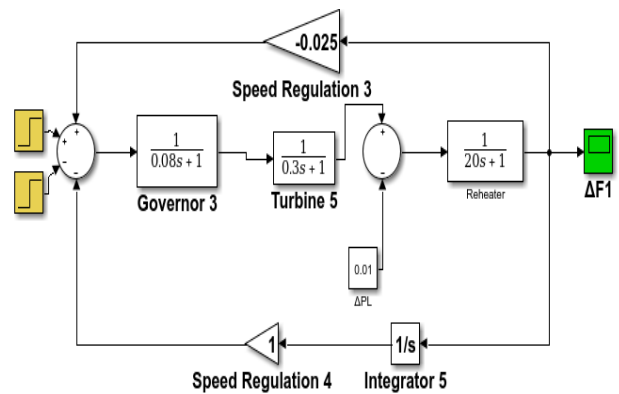


Fig. 3(a) Block Diagram representation of Single Area with SIMULINK Tool Box [4]

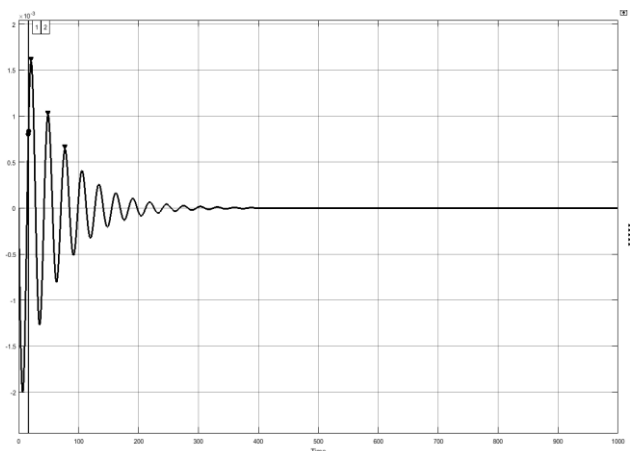


Fig. 3(b) Output/Images of Fig. 3(a) [4]: Deviation/Drop of frequency during power flow

2.1.1. Fig. 4(a) shows the block diagram representation of another model [4] with the use of SIMULINK Tool Box. Fig. 4(b) shows the output (Δf) of Fig. 4(a), the response shows transients continue up to 350 seconds and the steady state value is zero which implies proper control of LFC so that the frequency remains at its nominal value.

2.2. Model of “Load Frequency Control of single area/two area power system using Conventional and Intelligent Control”, [6] is considered. Fig. 5(a) shows the block diagram representation using SIMULINK Tool Box. Fig. 5(b) shows the output (Δf) of Fig. 5(a) [6], the response shows a transient continues up to 6 seconds and the steady state value is zero which implies proper control of LFC so that the frequency remains at its nominal value.

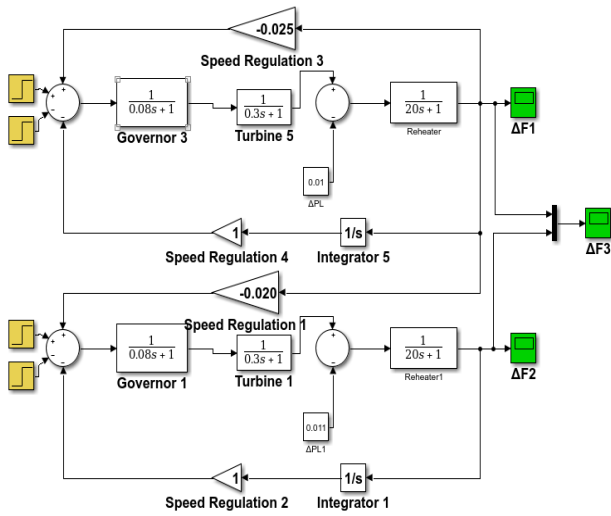


Fig. 4(a) Model of Implementation of GUI for Double Area LFC with SIMULINK Tool Box [4]

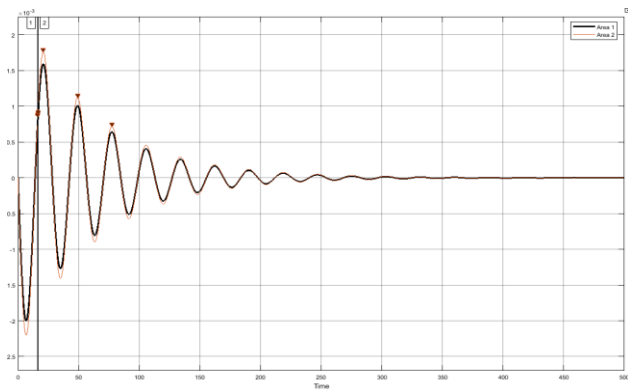


Fig. 4(b) Results / Images of Fig. 4(a) [4]: Deviation/Drop of frequency during power flow

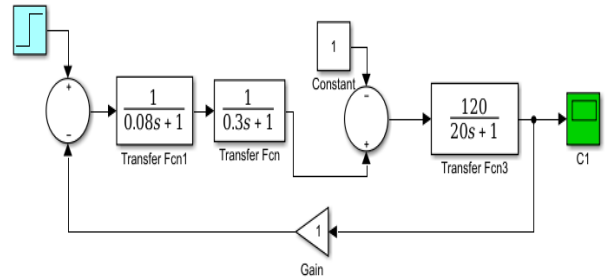


Fig. 5(a) Load Frequency Control of single area power system using conventional and Intelligent Control [6]

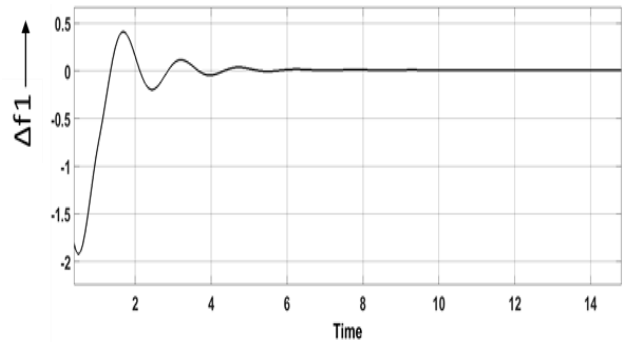


Fig. 5(b) Output of Fig. 5(a): Deviation/Drop of frequency during power flow

2.2.1 Model of two area power system [6] is shown in Fig. 6(a) with SIMULINK Tool Box. Fig 6(b) shows the output (Δf) of Fig. 6(a), the response shows transients continue up to 50 seconds and the steady state value is zero which implies proper control of LFC, so that the frequency remains at its nominal value.

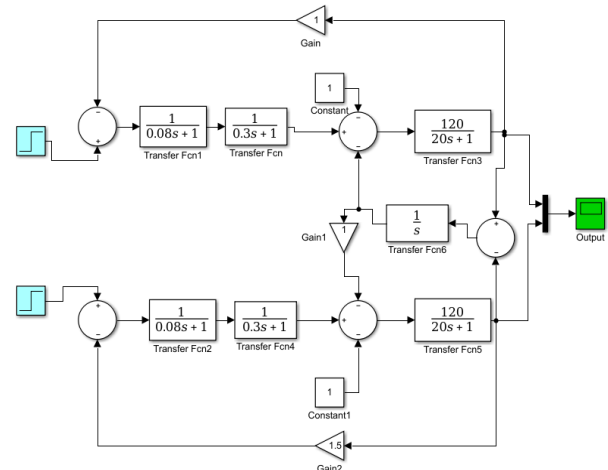


Fig. 6(a) Load Frequency Control of two area power system using conventional and Intelligent Control [6]

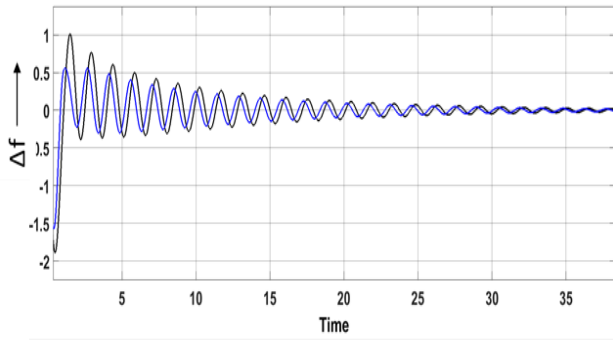


Fig. 6(b) Output of Fig. 6(a): Deviation/Drop of frequency during power flow

2.3. Model of “Robust PID controller for Load Frequency Control of Single Area, Re-heat Thermal Power Plant using Elephant Herding Optimization Techniques”, [8] is considered. Fig. 7(a) shows the block diagram representation using SIMULINK Tool Box. Fig. 7(b) shows the output (Δf) of Fig. 7(a), the response shows a transient continues up to 8 seconds and the steady state value is zero, which implies proper control of LFC so that the frequency remains at its nominal value without drop.

2.3.1 Fig. 8(a) shows the Double area model [8]. Fig. 8(b) shows the output (Δf) of Fig. 8(a), the response shows the transients continue up to 18 seconds and the steady state value is zero which implies the proper control of LFC, so that the frequency remains at nominal value without drop.

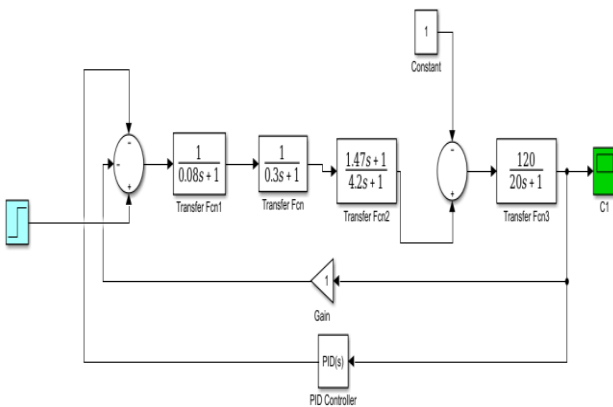


Fig. 7(a) Robust PID Controller for LFC of Single Area Reheat Thermal Power Plant using Elephant Herding Optimization Technique [8]

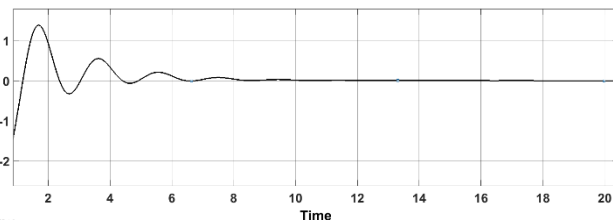


Fig. 7(b) Results / Images of Fig. 7(a) [8]: Deviation/Drop of frequency during power flow

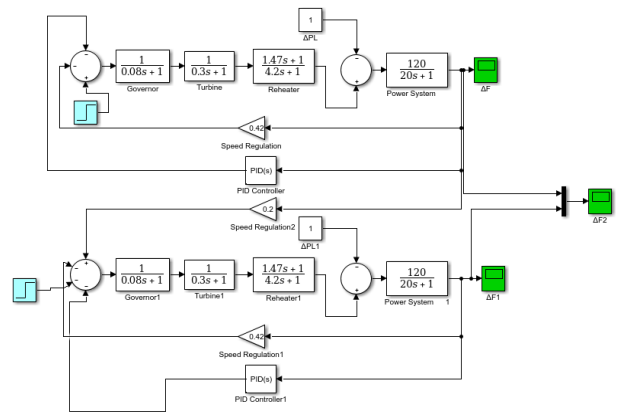


Fig. 8(a) Robust PID Controller for LFC of Double Area Reheat Thermal Power Plant using Elephant Herding Optimization Technique [8]

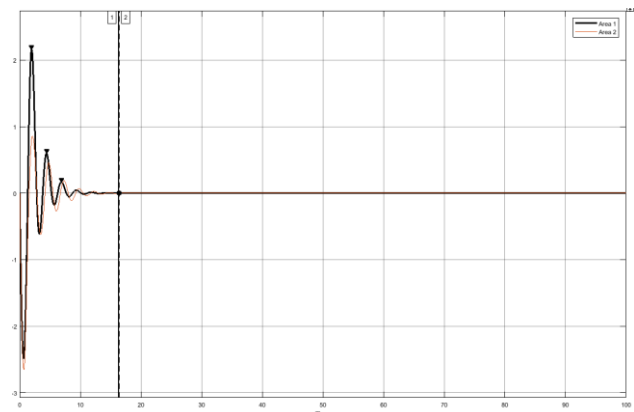


Fig. 8(b) Results / Images of Fig. 8(a) [8]: Deviation/Drop of frequency during power flow

2.4. Model of “Load Frequency control of inter connected power system with governor backlash nonlinearities”, [16] is considered. Fig. 9(a) shows the block diagram representation using SIMULINK Tool Box. Fig. 9(b) shows the output (Δf) of Fig. 9(a), the response shows the transients continue up to 18 seconds and the steady state value is zero, which implies proper control of LFC so that the frequency remains at its nominal value without drop.

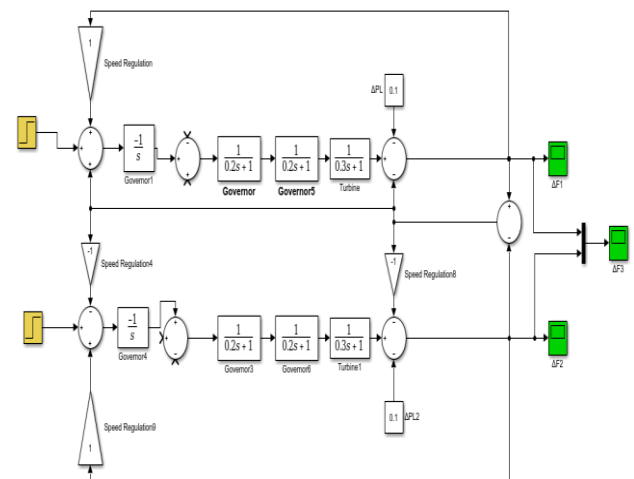


Fig. 9(a) Model for LFC of Interconnected Power System with Governor Backlash Nonlinearities [16]

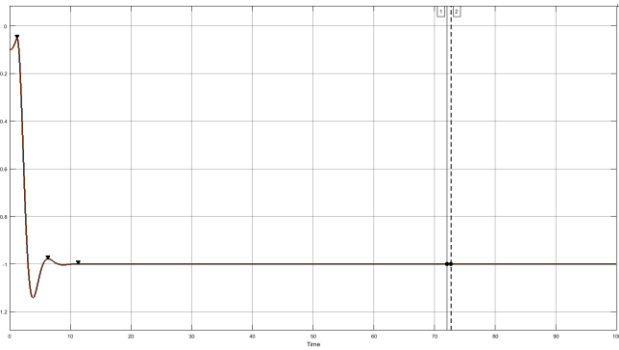


Fig. 9(b) Results / Images of Fig. 9(a) [16]: Deviation/Drop of frequency during power flow

3 Determination of Limit Cycles (LC)

The exhibition of LCs are determined for all models considered in section 2. Now the governor with Dead band/Backlash along with turbine and generator are tested.

3.1. The Fig. 3(a) [4] is considered and the existence of LC is determined under the autonomous state using SIMULINK Tool Box as shown in Fig. 10 (a) and the results / images of LC are shown in Fig. 10(b). The frequency of LC is 0.16 rad/sec noted.

3.1.1. The Fig. 4(a) [4] is considered and the existence of LC is determined under the autonomous state using SIMULINK Tool Box as shown in Fig. 11(a) and the results / images of LC are shown in Fig. 11(b). The frequency of LC is 0.16 rad/sec noted.

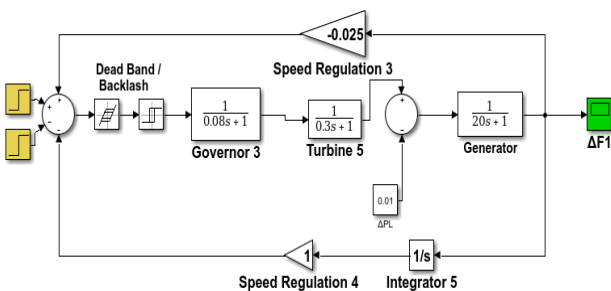


Fig. 10(a) Model of Implementation of GUI for Single Area LFC [4]

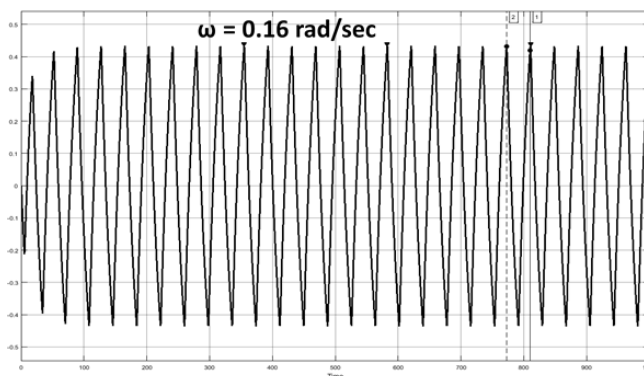


Fig. 10(b) Result/Image of 10(a) [4]: Prediction of LC

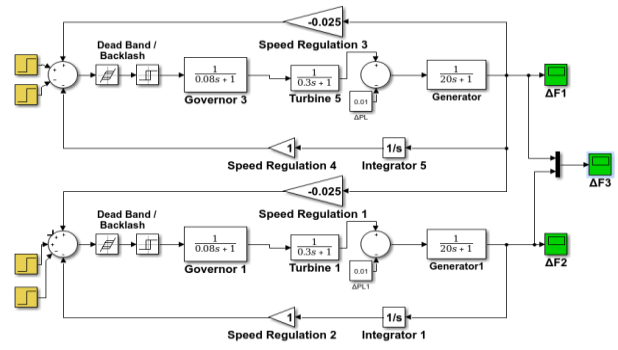


Fig. 11(a) Model of Implementation of GUI for Double Area LFC [4]

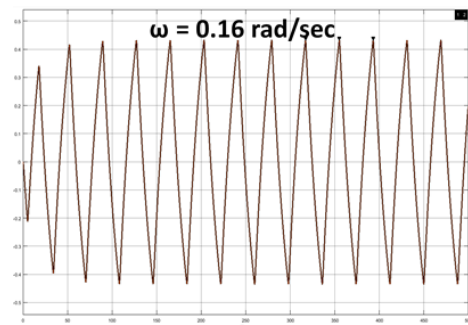


Fig. 11(b) Result/Image of 11(a) [4]: Prediction of LC

3.2. The Fig. 6(a) is considered and exhibition of LC is determined under autonomous state, using the SIMULINK Tool Box as shown in Fig. 12(a) and results/images of LC are shown in Fig. 12(b), the frequency of which is noted as 2.4 rad/sec.

3.2.1 The Fig. 6(a) is considered and exhibition of LC is determined under autonomous state, using the SIMULINK Tool Box as shown in Fig. 13(a) and results/images of LC are shown in Fig. 13(b), the frequency of which is noted as 2.4 rad/sec.

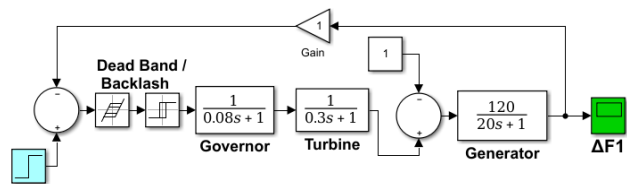


Fig. 12(a) Prediction of LC for Load Frequency Control of single area power system using conventional and Intelligent Control [6]

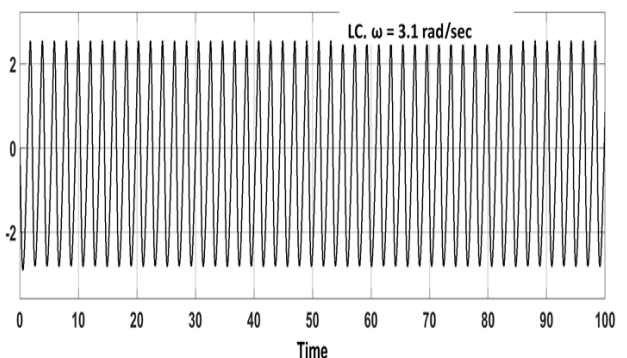


Fig. 12(b) Result/Image of 12(a) [6]: Prediction of LC

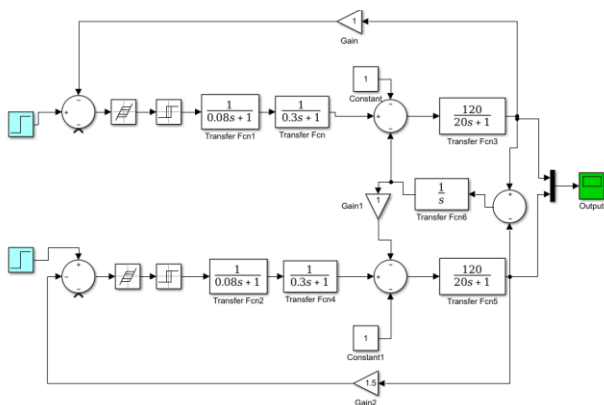


Fig. 13(a) Model for Load Frequency Control of two area power system using conventional and Intelligent Control [6]

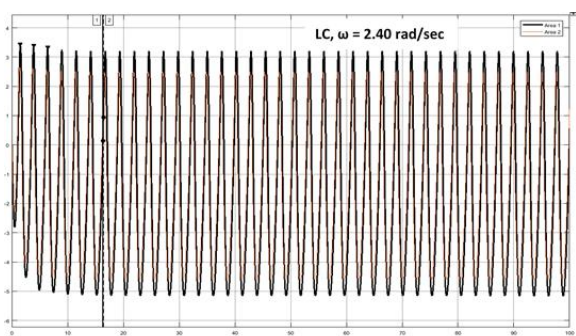


Fig. 13(b) Result/Image of Fig. 13(a) [6]: Prediction of LC

3.3 The Fig. 7(a) [8] is considered and the exhibition of LC is determined under autonomous state, using the SIMULINK Tool Box as shown in Fig. 14(a) and the results/images of LC are shown in Fig. 14(b), the frequency of which is noted as 2.2 rad/sec.

3.3.1 The Fig. 7(a) [8] is considered and the exhibition of LC is determined under autonomous state, using the SIMULINK Tool Box as shown in Fig. 15(a) and the results/images of LC are shown in Fig. 15(b), the frequency of which is noted as 1.58 rad/sec.

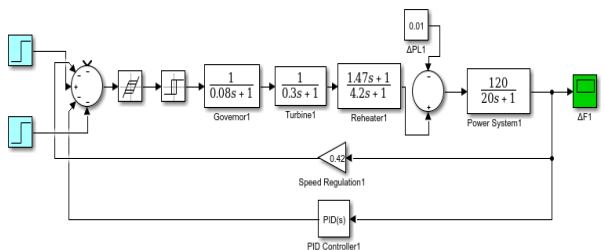


Fig. 14(a) Block Diagram Representation of Robust PID controller for LFC single area Reheat Thermal Power Plant using Elephant Herding Optimization Technique, Governor with Backlash Nonlinearity [8]

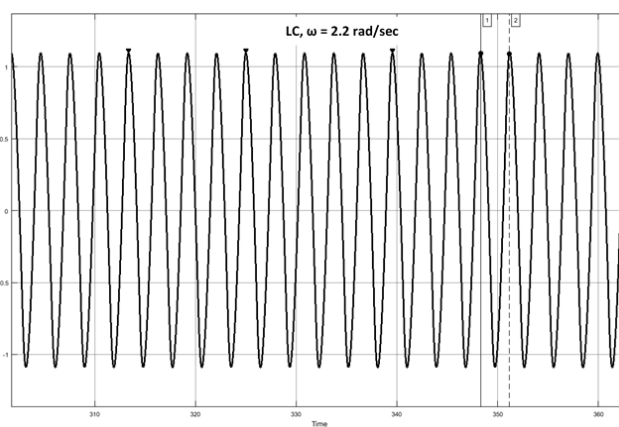


Fig. 14(b) Results / Images of Fig. 14(a)[8]: Prediction of LC

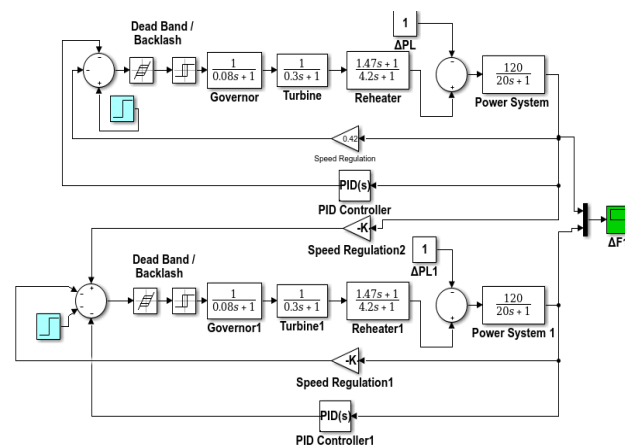


Fig. 15(a) Block Diagram Representation of Robust PID controller for LFC double area Reheat Thermal Power Plant using Elephant Herding Optimization Technique, Governor with Backlash Nonlinearity [8]

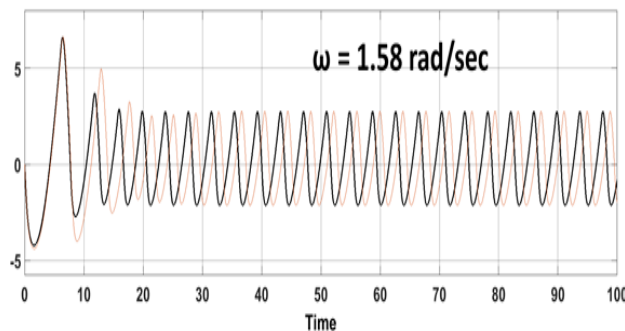


Fig. 15(b) Results / Images of Fig. 15(a) [8]: Prediction of LC

3.4 The Fig. 9(a) [16] is considered and the exhibition of LC is determined under autonomous state, using the SIMULINK Tool Box as shown in Fig. 16(a) and the results/images at LC are shown in Fig. 16(b), the frequency of which is noted as 0.90 rad/sec.

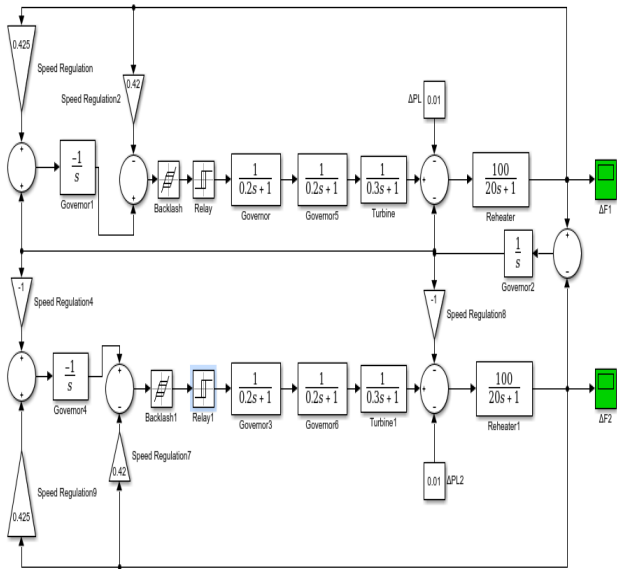


Fig. 16(a) Block Diagram representation of LFC with Governor Backlash Nonlinearities using SIMULINK Tool Box [16]

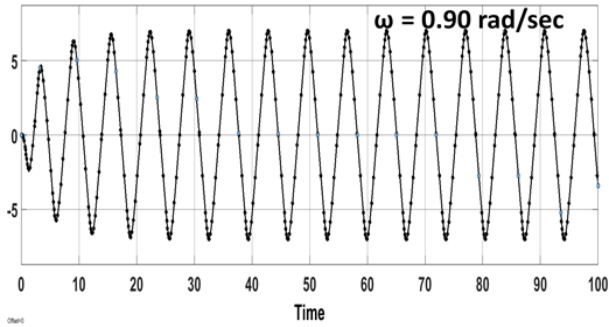


Fig. 16(b) Results/Images of Fig. 16(a) [16]: Prediction of LC

4 Signal Stabilization

All the models tested in section 3 exhibits LC/self-sustained oscillations. Quenching of such oscillations can be done by a method of signal stabilization [34, 37, 42, 44, 46], where a high frequency signal preferably at least 10 times the frequency of LC is injected at any point of the system.

As a result, the LC is completely quenched and the system will be synchronized to the frequency of forcing stabilizing signal.

4.1 Fig. 17(a) shows the signal stabilization of the model shown Fig. 2.1[4] using the stabilizing signal $U \sin \omega t$, where $U=6$, $\omega = 2$ rad/sec.

Fig. 17(b) shows the results/images of Fig. 17(a) where the frequency of synchronized signal is noted as $\omega = 1.98$ rad/sec.

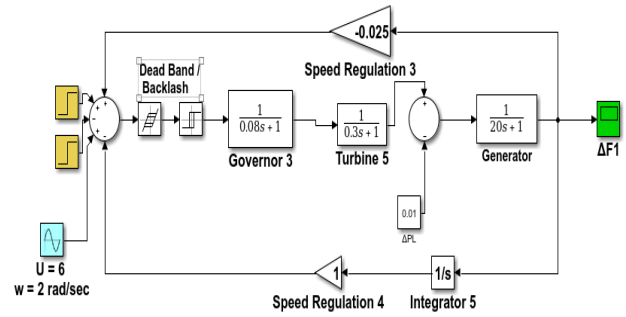


Fig. 17(a) Block Diagram representation of Signal Stabilization of the model shown in Fig. 3(a) [4]

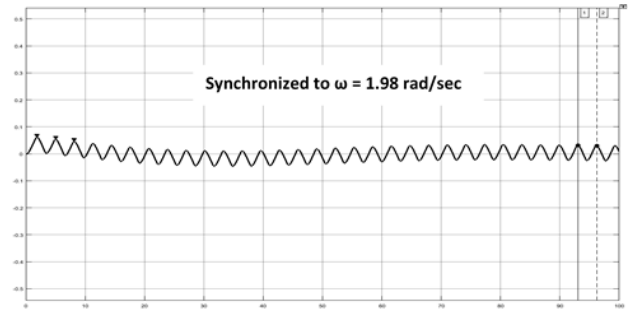


Fig. 17(b) Results/Images of Fig. 17(a) [4]: Prediction of LC

4.1.1 Fig. 18(b) shows the results/images of Fig. 18(a) where the frequency of synchronized signal is noted as $\omega = 2.01$ rad/sec.

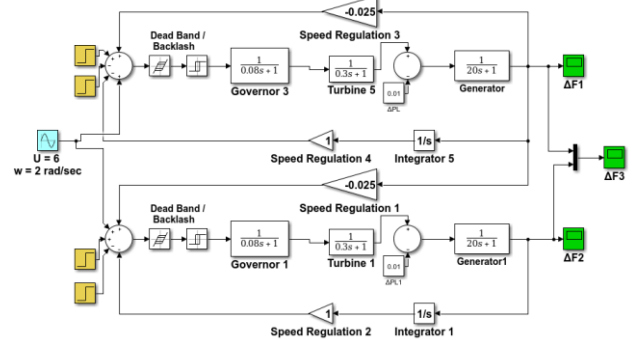


Fig. 18(a) Block Diagram representation of Signal Stabilization double area of the model shown in Fig. 3(a) [4]

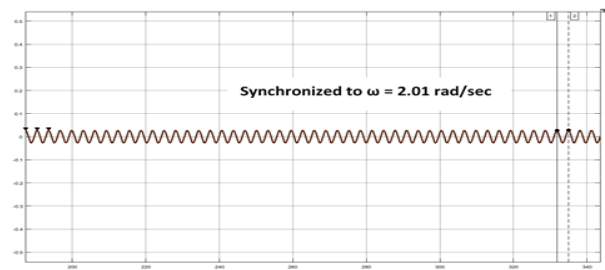


Fig. 18(b) Results/Images of Fig. 18(a) [4]: Signal Stabilization

4.2 Fig. 19(a) shows the signal stabilization of the model shown in Fig. 6 [6] using the stabilizing signal $U \sin \omega t$, where $U=6$, $\omega=31$ rad/sec. Fig. 19(b) shows the results/images of Fig. 19(a), where the frequency of synchronized signal is noted as $\omega = 30.6$ rad/sec.

4.2.1 Fig. 20(a) shows the signal stabilization of the model shown in Fig. 6 [6] using the stabilizing signal $U \sin \omega t$, where $U=5$, $\omega=24$ rad/sec. Fig. 20(b) shows the results/images of Fig. 20(a), where the frequency of synchronized signal is noted as $\omega = 23.01$ rad/sec.

4.3 Fig. 21 shows the signal stabilization of the model in Fig. 7 [8] the stabilizing signal is $U \sin \omega t$, $U=6$, $\omega=23$ rad/sec. Fig. 21(b) Shows the results/images of Fig. 21(a), where the frequency of synchronized signal in 22.8 rad/sec.

4.3.1 Fig. 22 shows the signal stabilization of the model in Fig. 7 [8] the stabilizing signal is $U \sin \omega t$, $U=6$, $\omega=16$ rad/sec. Fig. 22(b) Shows the results/images of Fig. 22(a), where the frequency of synchronized signal in 16.3 rad/sec.

4.4. Fig. 23(a) shows the signal stabilization of the Model shown in Fig. 9 [16]. The stabilizing signal is using, where $U=5$, $\omega=10$ rad/sec. Fig. 23(b) shows the results/images of Fig. 23(a) where the frequency of the synchronized signal is 9.38 rad/sec.

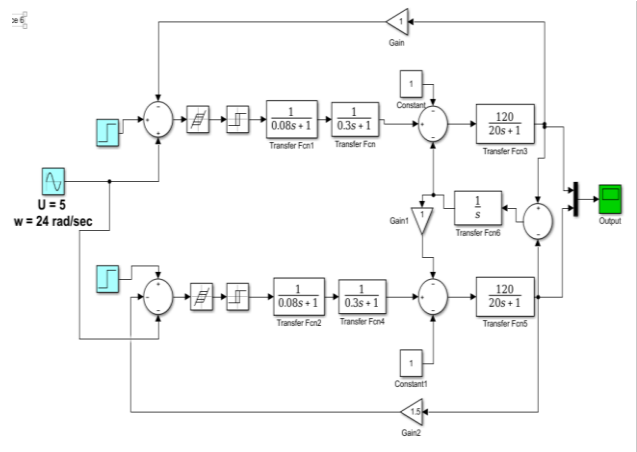


Fig. 20(a) Block Diagram representation of Signal Stabilization of the Model shown in Fig. 6(a) [6]

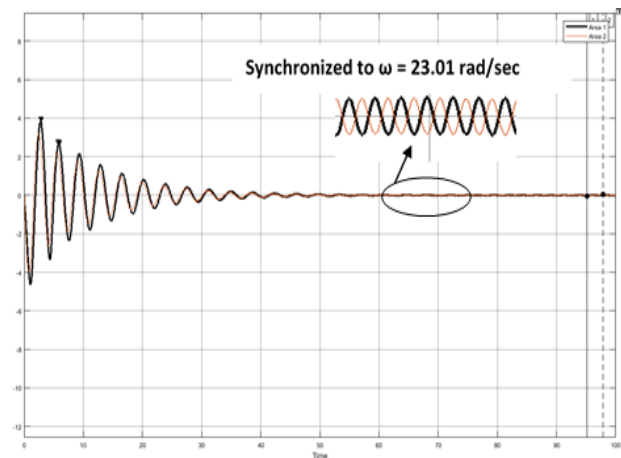


Fig. 20(b) Results/Images of Fig. 20(a) [6]: Signal Stabilization

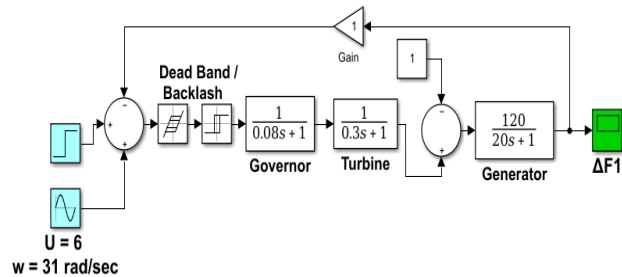


Fig. 19(a) Block Diagram representation of Signal Stabilization of the Model shown in Fig. 6(a) [6]

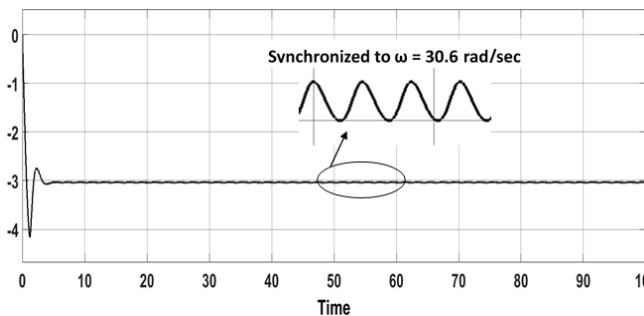


Fig. 19(b) Results/Images of Fig. 19(a) [6]: Signal Stabilization

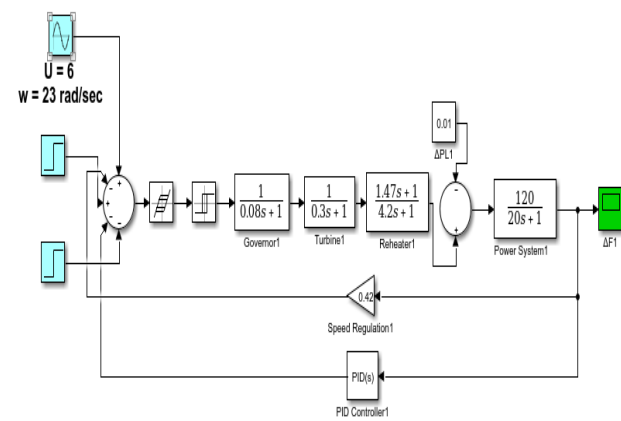


Fig. 21(a) Signal Stabilization of Robust PID controller for LFC single area Reheat Thermal Power Plant using Elephant Herding Optimization Technique, Governor with Backlash Nonlinearity [8]

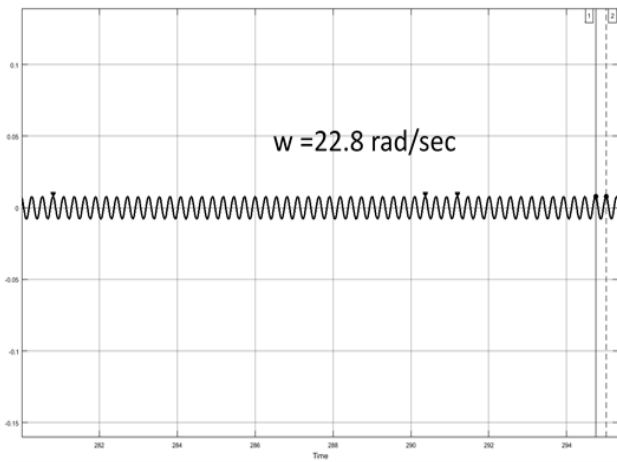


Fig. 21(b) Results/Images of Fig. 21(a) [8]: Signal Stabilization

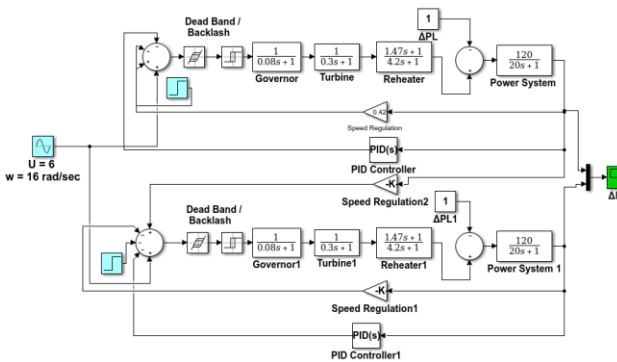


Fig. 22(a) Signal Stabilization of Robust PID controller for LFC double area Reheat Thermal Power Plant using Elephant Herding Optimization Technique, Governor with Backlash Nonlinearity [8]

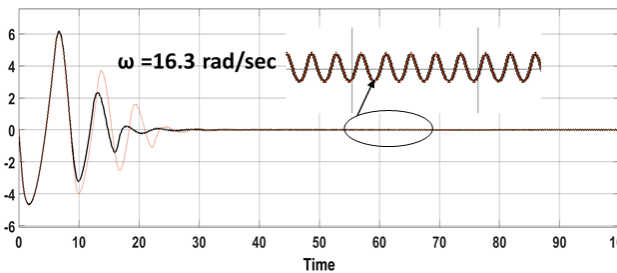


Fig. 22(b) Results/Images of Fig. 22(a) [8]: Signal Stabilization

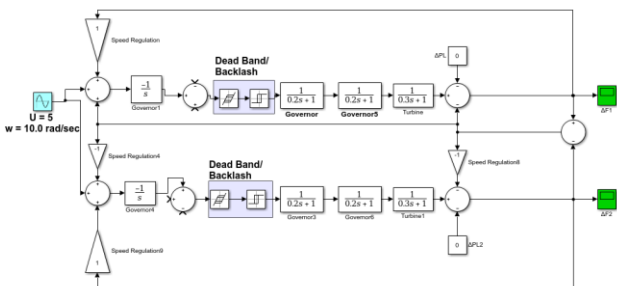


Fig. 23(a) Signal Stabilization of LFC with Governor Backlash Nonlinearities [16]

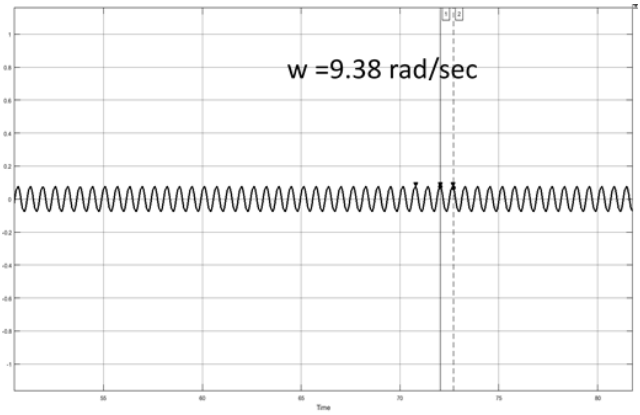


Fig. 23(b) Results/Images of Fig. 23(a) [16]: Signal Stabilization

5 Digital Controller with Deadbeat Approach

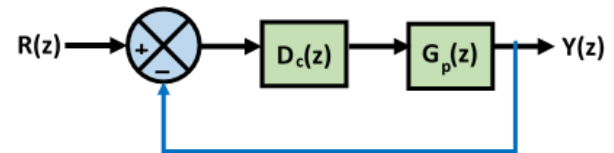


Fig. 24: A simple model of a Digital Controller

$$M(z) = \text{Closed loop transfer function} = \frac{Y(z)}{R(z)} = \frac{1}{z^n}$$

in order to have deadbeat response [47].

where n=No. of excess poles than zeroes.

In the signal stabilization the input is $U \sin \omega_f t$ as shown in Fig. 24 at the point R(z).

$$Z[U \sin \omega_f t] = \frac{U z \sin \omega_f T}{z^2 - 2z \cos \omega_f T + 1}, \text{ here } n=1.$$

Hence $\frac{1}{z^n} = \frac{1}{z^1} = z^{-1}$. In the use of SIMULINK Toolbox a z^{-1} signal to be multiplied with the stabilized / synchronized output as shown in Fig. 25(a) and 26(a). The results/images are shown in Fig. 25(b) and Fig. 26(b).

5.1 Fig. 25(a) is the block diagram representation of signal stabilization with deadbeat control [4]. Fig. 25(b) shows the results /images of Fig. 25(a) which shows the transient free, ripple free, with zero steady state error and within the least time response is obtained. So it is highly suitable for real time applications.

5.1.1 Fig. 26(a) is the block diagram representation of signal stabilization with deadbeat control [4]. Fig. 26(b) shows the results/images of Fig. 26(a) which shows the transient free, ripple free, with zero steady state error and within the least time response is obtained. So, it is the highly suitable for real time applications.

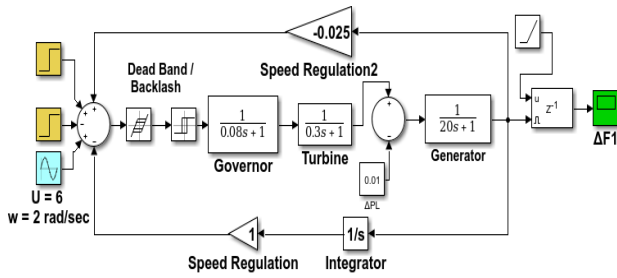


Fig. 25(a) Block Diagram representation of Signal Stabilization with dead beat control [4]

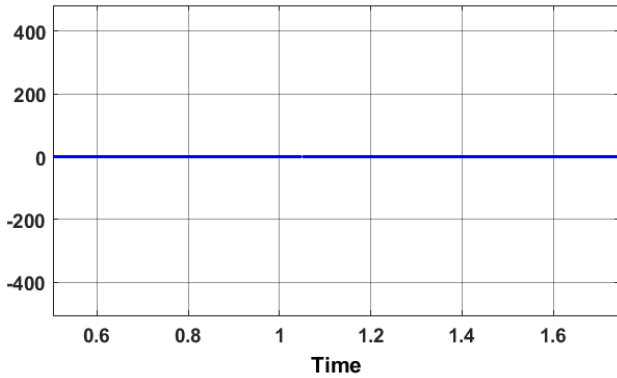


Fig. 25(b) Results/Images of Fig. 25(a) [4]: Deadbeat Controller

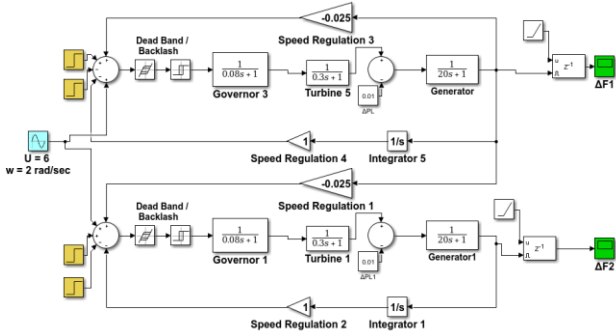


Fig. 26(a) Block Diagram representation of Signal Stabilization double area with deadbeat control [4]

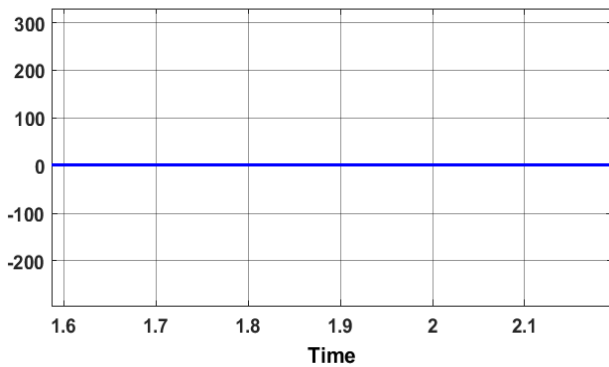


Fig. 26(b) Results/Images of Fig. 26(a) [4]: Deadbeat Controller

5.2 Fig. 27(a) is block diagram representation of signal stabilization of Fig. 6(a) with dead beat control [6]. Fig. 27(b) shows the results/images of Fig. 27(b) which shows the transient free, ripple free, with zero steady state error and within least time (almost zero time) response is obtained so it is highly suitable for real time applications.

5.2.1 Fig. 28(a) is block diagram representation of signal stabilization of Fig. 6(a) with deadbeat control [6]. Fig. 28(b) shows the results/images of Fig. 28(a) which shows the transient free, ripple free, with zero steady state error and within least time (almost zero time) response is obtained so it is highly suitable for real time applications.

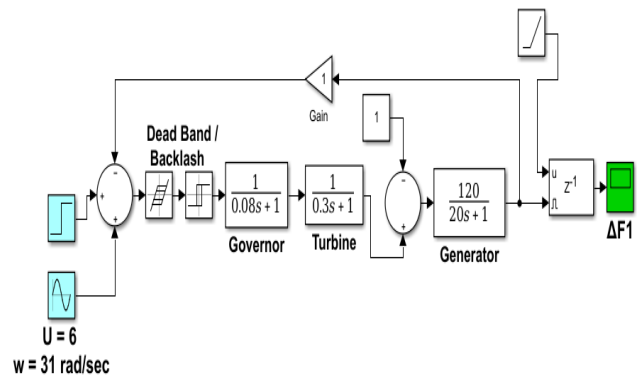


Fig. 27(a) Block Diagram Representation for Signal Stabilization with Deadbeat Approach [6]

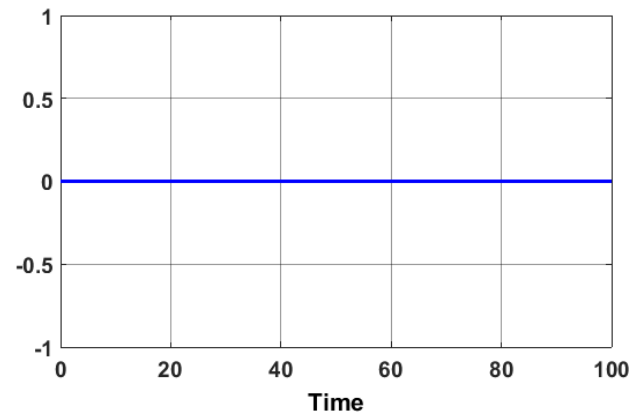


Fig. 27(b) Results/Images for Fig. 27(a) [6]: Deadbeat Controller

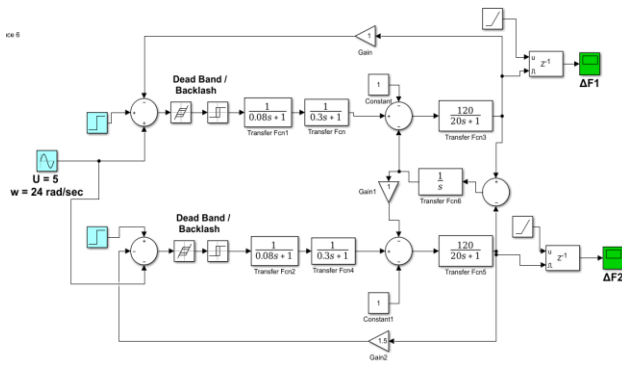


Fig. 28(a) Block Diagram Representation for Signal Stabilization with Deadbeat Approach [6]

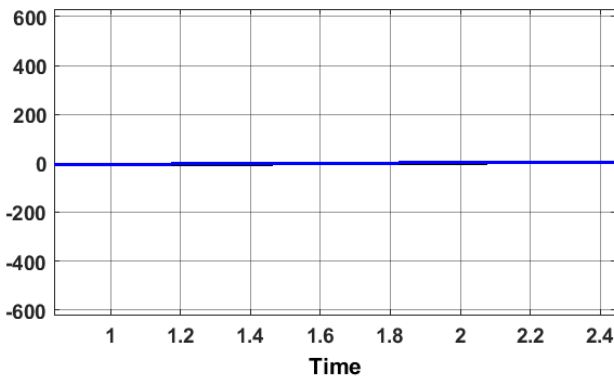


Fig. 28(b) Results/Images for Fig. 28(a) [6]: Deadbeat Controller

5.3 Fig. 7(a) is block diagram representation of signal stabilization of Fig. 29(a) with deadbeat control, [8], Fig. 29(b) shows the results/images of Fig. 29(a) where the transient free, ripple free, with no steady state error and within least time (almost zero time) response is obtained. So it is highly suitable for real time applications.

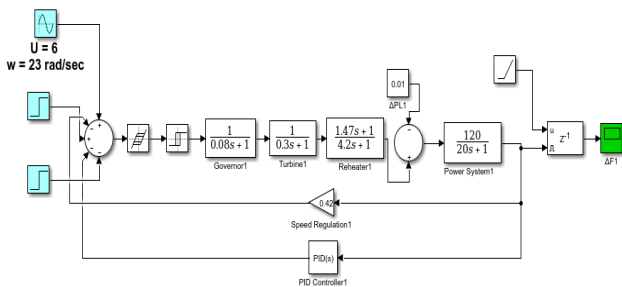


Fig. 29(a) Block Diagram Representation for Signal Stabilization with Deadbeat Approach [8]

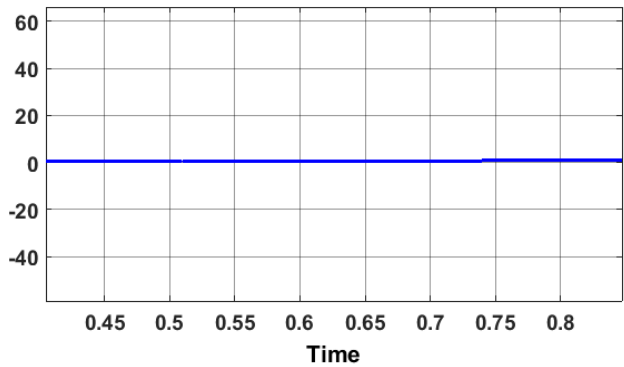


Fig. 29(b) Results/Images for Fig. 29(a) [8]: Deadbeat Controller

5.3.1 Fig. 7(a) is block diagram representation of signal stabilization of Fig. 30(a) with dead beat control, [8], Fig. 30(b) shows the results/images of Fig. 30(a) where the transient free, ripple free, with no steady state error and within least time (almost zero time) response is obtained. So it is highly suitable for real time applications.

5.4 Fig. 31(a) is block diagram representation of signal stabilization with deadbeat control of the model of Fig. 9(a) [16]. Fig. 31(b) shows the results/images of 31(a) where the transient free ripple free, with no steady state error, response is obtained. So it is highly suitable for real time applications.

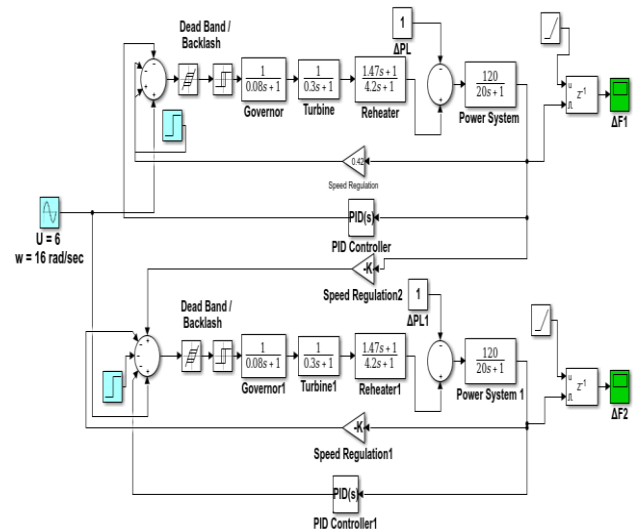


Fig. 30(a) Block Diagram Representation for Signal Stabilization with Deadbeat Approach [8]

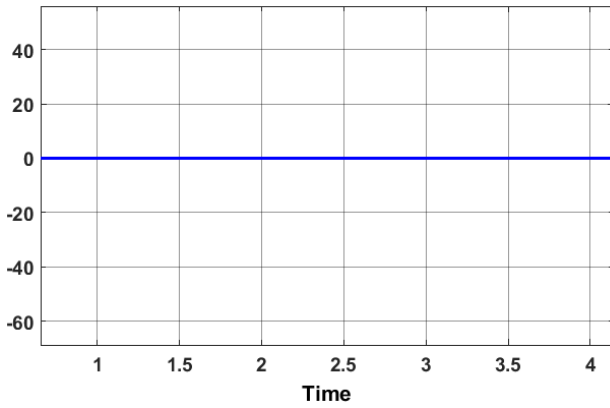


Fig. 30(b) Results/Images for Fig. 30(a) [8]: Deadbeat Controller

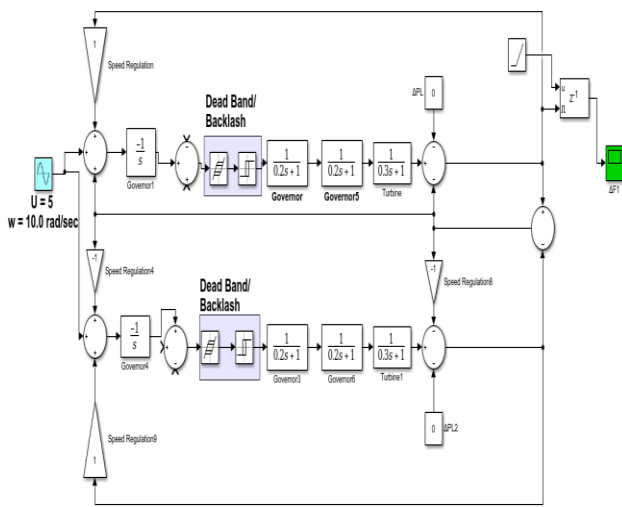


Fig. 31(a) Signal Stabilization with Deadbeat Control of LFC with Governor Backlash Nonlinearities [16]

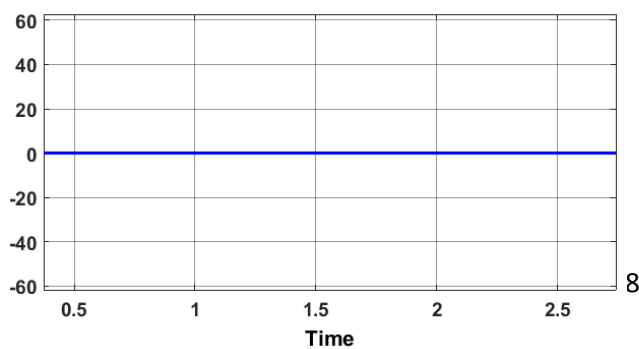


Fig. 31(b) Results/Images of Fig. 31(a) [16]: Deadbeat Controller

A comparative table showing the response time for steady state value of Δf using different approaches from different cases with the present work.

Table: Comparison of Response Time to Reach Steady-State for Δf Using Different Controller Approaches

Sl. No.	Cases	Controller Type	Methodology /Approach	Response Time for Steady State value of Δf	Complete Quenching/ Complete Mitigation of	Remark
1	Implementation of graphical user interface for single area load frequency control [4]	PI	Single Area	350 s	No	
2	Load Frequency control of Two Area Interconnected Power system using conventional and Intelligent controllers [6]	Intelligent	Single Area	6 s	No	
			Double Area	50 s		
3	A Robust PID controller for load frequency control of single area reheat Thermal Power Plant using Elephant Herding Optimization Techniques [8]	Robust PID	Single Area	10 s	No	
			Double Area	18 s		
4	Load frequency control of interconnected power system with Governor backlash nonlinearities [16]	Integrator gains of supplementary controllers	Double Area	18 s	No	
5	Load Frequency Control by Speed Governors of Two-Area Power System using Digital Controller with Deadbeat Approach (present work)	Digital Controller with Deadbeat Approach	All models tested with the proposed four steps procedure	0.0 s	Yes	All the models cited in Sl. No. 1, 2, 3, 4 have been tested through proposed 4 step procedures

6 Conclusion

After examining and testing several models, we reached the conclusive decision to focus on a two-area interconnected power system, where each area consists of a turbine, generator, and governor. Using simulations with the SIMULINK Toolbox, we analyzed the steady-state responses for both single-area and two-area systems. By implementing a digital controller combined with a deadbeat

approach, we demonstrated that the limit cycles (LC) caused by the inherent dead band/backlash nonlinearity in governors can be effectively quenched through signal stabilization using a high-frequency signal—specifically, at least 10 times the LC frequency. This enables precise and effective Load Frequency Control (LFC), maintaining system frequency at its nominal value.

The application of the digital controller with the deadbeat approach achieves a transient-free, ripple-free response with zero steady-state error and an almost instantaneous (near-zero time) response, making real-time control feasible.

Based on a thorough literature survey, it became clear that selected models comprising turbine, generator, and governor should be examined and tested systematically. Four sequential tests were conducted on all selected models.

First test has been conducted with the models comprising of Turbine, Generator, Governor without the nonlinearity. This was conducted only steady state response were observed to ensure the performance capability of LFC. Second test was conducted under an autonomous state on all models.

In the 2nd test the exhibition of LC was detected and their frequencies were noted so that in the 3rd test the frequency stabilizing signal to be taken at least 10 times the frequency LC. Third test of signal stabilization taking at least 10 times the frequency of LC have been conducted on the model and observed the systems were synchronized to their respective forcing stabilizing signal frequency.

Fourth test have been conducted on models having nonlinearity present, the stabilizing signal with digital deadbeat control. The results of all the models show, transient free, ripple free with no steady state error, the least time (almost zero time) response which facilitates the real time application.

The novelty of this work lies in the complete elimination of sustained oscillations, the achievement of the fastest response times, and the practical implementation of a deadbeat digital controller that enables real-time LFC applications. The proposed four-step procedure can be extended to more complex power system models incorporating Load Frequency Control in future.

Acknowledgment

The authors wish to thank the C.V. Raman Global University, Bhubaneswar – 752054, Odisha, India, for providing computer facilities for the preparation of this paper.

References

- [1] Gulzar, M.M., Iqbal, M., Shahzad, S., Muqeet, H.A., Shahzad, M., Hussain, M.M., Load Frequency Control (LFC) Strategies in Renewable Energy-Based Hybrid Power Systems: A Review, *Energies*, 15, 2022, 3488.
- [2] Kothari, D.P., Nagrath, I, et al., *Modern Power System Analysis*. Tata McGraw Hill Education, 2011.
- [3] Kundur, P, Batu, N. J and Lauby, M.G., *Power System stability and control*. McGraw-Hill New York, 1994.
- [4] Wagh, S and Choubey, S., Implementation of graphical user interface for single area load frequency control, IEEE 1st International conference in Electronics, *Materials Engineering & Nano-Technology*, 2017.
- [5] Alhalabi, M, Rashed, A. et al., Two-area Load Frequency control for power system Dynamic Performance Enhancement with Graphic User Interface Integration, *Proc. Of the International conference on Electrical computer and Energy Technologies (ICECET2022)*, 20-22, 2022.
- [6] Vavilala, S. K, Srinivas, R.S, et al., Load Frequency control of Two Area Interconnected Power system using conventional and Intelligent controllers, *Journal of Engineering Research and Applications*, ISSN: 2248-9622, vol.4, 2014, pp 156-160.
- [7] Moghaddam, S.G, Bagheri, A. A, et. al., Load Frequency control in a Two-area Power system using the Fuzzy-PID Method, *ECTI Transactions on Electrical Engineering, Electronics and Communications*, vol. 21, No.1, 2023.
- [8] Sambariya, D. K and Fagna, R, A Robust PID controller for load frequency control of single area re-heat Thermal Power Plant using Elephant Herding Optimization Techniques, IEEE, *International Conference on Information, Communication and Control (ICICIC -2017)* Paper Id: 279.
- [9] Turk, Ismail, Kilic, H, et al., Robust Load Frequency Control in Hybrid Micro grids using Type-3 Fuzzy Logic under stochastic variations, *Symmetry (MDPI)* 17, 2025, 853.
- [10] Maurya, A. K., and Khan, H., Comprehensive Analysis of Load Frequency Control in Multi-area of Power System Networks, *AKGEC International Journal of Technology*, Vol. 15. No 2.
- [11] Thotakura, N.L, Burge, C.R, et al., Impact of the Exciter and Governor Parameters on Forced

- Oscillation, *Electronics* (MDPI), 13, 2024, 3177
<http://doi.org/10.3390>
- [12] Tungadio, D.H and Sun, Y, Load Frequency Controllers considering renewable energy integration in power system, *Energy Report Elsevier*, 5, 2019, 436-453.
- [13] Wang, L, Model Predictive Control System Design and Implementation using MATLAB, *Springer*, 2009
- [14] Elsisst, M, et al, Bat inspired algorithm based optimal design of model predictive load frequency control, *Int J Electro Power Energy System*. 83, 2016, 426-433.
- [15] Zheng, V., et al., A distributed Model predictive control based load frequency control scheme for inter connected power system using discrete time Laguerre functions, *ISA Trans*, 68, 2017, 127-140.
- [16] Tsay, T. S., Load frequency control of interconnected power system with Governor backlash nonlinearities, Elsevier, *Electrical Power and Energy System* 33, 2011, 1542-1549.
- [17] Chidambaram, I.A., Velusami, S., Decentralized Biased controllers for Load-Frequency control of Inter connected Power Systems considering Governor Dead Band Non-linearity, *IEEE Indicon, 2005 conference*, 2005, page 1599.
- [18] Tripathy SC, Hop GS, Malik Op., Optimization of load-frequency control parameters for power system with reat steam turbines and governor dead-band nonlinearity, *PROC IEE ptc*, 1982, 129(1), 10-6.
- [19] Tripathy SC, Balasubramanian R, Nair PSC, Effect of superconducting magnetic energy storage on automatic generation control considering governor dead-band and boiler dynamics, *IEEE Trans Power Syst*, 7(3), 1992, 1266-73.
- [20] Lu CF, Liu CC, WU CJ, Effect of battery energy storage system on load frequency control considering governor dead-band and generation rate constraint, *IEEE Trans Energy Convers*, 1995, 10(1), 555-61.
- [21] Kumar A. Malik O.P. Hope GS., Variable-structure-system control applied to AGC of an interconnected power system, *IEE Proceedings C (Generation, Transmission and Distribution)*, 1985,132(1), 23-29.
- [22] Kumar A, Malik O.P., Hope GS, Discrete variable structure controller for load frequency control of multi area interconnected power systems, *IEE Proceedings C (Generation, Transmission and Distribution)* 1987, 134(2),116-122.
- [23] Yang MS., Decentralized sliding mode stabilizer design for multi-area interconnected power systems, *In: Proceedings of the 2000 IEEE international symposium on industrial electronics*, vol. 1: 2000, p.185-190.
- [24] Aideen M. Marsh J.F., Decentralized proportional – plus-integral design method for interconnected power systems, *IEE Proceedings C (Generation, Transmission and Distribution)*, 1991, 138(4), 263-274.
- [25] Khodabakhshian A. Hooshmand R., A new PID controller design for automatic generation control of hydro power system., *Int J Elect Power Energy Syst* 2010, 32(5), 375-82.
- [26] Alrifai MT. Hassan MF. Zribi M., Decentralized load frequency controller for a multi-area interconnected power system, *Int J Electr power Energy syst*, 211, 33(2), 198-209.
- [27] Tan W., Tuning of PID load frequency controller of power systems, *Energy Convers Manage* 2009, 50(6), 1465-1472.
- [28] Juang C.F. Lu CF., Power System load frequency control by evolutionary Fuzzy PI Controller, *IEEE International Conference on Fuzzy Systems*, 2004. P. 715-719.
- [29] Kocaarsian I. Cam E., Fuzzy logic controller in interconnected electrical power systems for load-frequency control, *Int J Electri power Energy Syst* 2005, 27(8), 542-549.
- [30] Mathur H.D. Manjunath HV., Extended fuzzy logic based integral controller for three area power system with generation rate constraint, *In: ICIT 2006 IEEE international conference on industrial technology*, 2006, p.917-921.
- [31] Moon, Y.H and et al., Extended integral control for load frequency control with the consideration of generation rate constraints, *International Journal of Electrical power & Engg. Systems*, vol.24, Issue 4, 2002. pp 263-269.
- [32] Tsay TS, Han KW., Limit cycle analysis of nonlinear multivariable feedback control systems, *J Franklin Inst* 1988, 325(6), 721-30.
- [33] Atherton DP, Spurgeon S., Nonlinear control systems, analytical methods, *Electrical engineering encyclopedia*. New York: John Wiley & Sons. Inc.:1999.
- [34] Patra KC, Singh Y.P., Graphical method of prediction of limit cycle for multivariable nonlinear systems. *IEE PROC control Theory Appl* 1996, 143(5), 423-428.
- [35] Gray J.O, Taylor P.M., Computer aided design of multivariable nonlinear control system using frequency domain techniques, *Automatica* 1979, 5, 281-297.
- [36] Gray J.O Nakhla NB., Prediction of limit cycle in multivariable nonlinear systems, *PROC IEE PtD* 1981, 128(5), 238-241.
- [37] Patra, K.C, Kar, N., Suppression Limit Cycles in 2x2 nonlinear systems with memory type nonlinearities. *International Journal of Dynamics and Control, Springer Nature*, 34, 95, vol. 10 Issue 3, 2022, pp 721-733.

- [38] Ashtaq, T, Muntaz, S, and et al, Automatic Generation Control is Renewables Integrated Multi-Area Power systems: A comparative Control Analysis, *Sustainability*, 16, 2024, 5735
- [39] Jain, D., et al., Comprehensive review on control systems and stability investigation of hybrid AC-DC micro grid, *Electrical Power System*, Res 2021, 45, 14085-140116
- [40] Bevrani, H., Golpira, H., and et al, Power system frequency control: An updated review of current solutions and new challenges, *Elew. Power syst. Res* 2021, 194, 107114
- [41] Parigrahi, D; and et al, A comprehensive review on intelligent I landing detection techniques for renewable energy integrated power system, *Int J . Energy Res* 2021, 45, 14085-14116.
- [42] Patra, K.C. and Dakua, B.K., Investigation of Limit Cycles and signal stabilization of two dimensional systems with memory type nonlinear elements, *Archivers of control sciences*, vol. 28, 285-330.
- [43] Wang, C., Yang, M., Zheng, W., Hu, K., and Xu, D. Analysis and suppression of limit cycle oscillation Nonlinearity, *IEEE Transactions on Industrial Electronics*, vol. 62,(12), 2017, 9261-9270
- [44] Patra, K.C., Pati, B.B., An Investigation of Forced Oscillations for Signal stabilization of Two Dimensional Nonlinear systems, *Systems & Control Letters*, Volume 35, Issue 4, 19 November 1998, 229-236
- [45] Patra, K.C., Patnaik, A., Estimation of Limit cycles and signal stabilization with dead beat approach in three dimensional. Nonlinear systems, *Int. J. of control system and Robotics*.
- [46] Oldenburger, R.T. Nakada, T. Signal stabilization of Self Oscillating System, *IRE Transactions on Automatic Control*, vol. 6, no. 3, 1961, 319-325.
- [47] Benjamin, C. Kuo, *Digital Control Systems*, Oxford Universities Press, 2nd Edition, 8th Impression, 2004.

Contribution of individual authors to the creation of a scientific article (ghostwriting policy)

Kartik Chandra Patra has formulated the problem, methodology of analysis adopted and algorithm of computation presented.

Asutosh Patnaik has made the validation of the results using the geometric tools and SIMULINK toolbox of MATLAB software.

Sources of funding for research presented in a scientific article or scientific article itself

No source of funding.

Conflict of Interest

The authors have no conflicts of interest to declare that are relevant to the content of this article.

Creative Commons Attribution License 4.0 (Attribution 4.0 International, CC BY 4.0)

This article is published under the terms of the Creative Commons Attribution License 4.0

https://creativecommons.org/licenses/by/4.0/deed.en_US